Impact of surface emissivity and atmospheric conditions on surface temperatures estimated from top of canopy brightness temperatures derived from Landsat 7 data

Albert Olioso, Maria Mira Sarrio, Dominique Courault, Olivier Marloie, Pierre Guillevic

IMPACT OF SURFACE EMISSIVITY AND ATMOSPHERIC CONDITIONS ON SURFACE TEMPERATURES ESTIMATED FROM TOP OF CANOPY BRIGHTNESS TEMPERATURES DERIVED FROM LANDSAT 7 DATA

Albert Olioso (1,2), Maria Mira (1,2,3), Dominique Courault (1,2), Olivier Marloie (4), Pierre Guillevic (5)

(1) INRA, EMMAH - UMR 1114, 84914 Avignon, France, [contact: olioso@avignon.inra.fr]
(1) UAPV (Université d'Avignon et des Pays de Vaucluse), EMMAH - UMR 1114, Avignon, France
(2) Cooperative Institute for Climate and Satellites (CICS), North Carolina State University, 151 Patton Avenue, Asheville, NC 28801, USA

ABSTRACT

The method to derive surface temperature from top of canopy brightness temperature developed by Olioso (1995b) [20] is tested over the Avignon-Crau-Camargue area (France) using Landsat-7 ETM+ images. The difference between surface temperature and brightness temperature depends on surface emissivity, incident atmospheric radiation and the temperature itself. Differences up to 2 K were obtained for a surface emissivity of 0.97. It can increase up to 7 K when surface emissivity was 0.91. The surface temperature derived from Landsat data were in agreement with the ground measurements when using local calibration of the surface emissivity derivation method and a modification of the calculation of atmospheric radiation as compared to [20]. The impact of error in emissivity derivation was higher than the impact of errors in deriving atmospheric radiation.

Index Terms— Surface temperature, thermal infrared, surface emissivity, atmospheric radiation

1. INTRODUCTION

Surface temperature is a key variable for monitoring land surface energy balance and in particular evapotranspiration ([2], [4], [5], [21], [28], [26], [24]). Remote measurement of surface temperature allows assessing surface energy balance at various spatial scales from satellite and airplane platforms or from hand-held thermal infrared radiometers. However, surface temperature cannot be directly derived from thermal measurements. Measured radiation includes not only the radiation emitted by the surface but also the radiation emitted by the atmosphere. If we consider top of canopy measurements, this additional radiation results from the reflection of atmospheric radiation by the surface toward the sensor. Impact of surface emissivity must also be accounted since it directly affects the level of emitted radiation at a given temperature. Poor knowledge in either surface emissivity or atmospheric radiation results in error in the determination of surface temperature from remote sensing measurement. These effects have been recognized for a long time (e.g. [5], [15], [25]). Olioso (1995b, [20]) showed that an error of +/- 0.01 on surface emissivity results in an error between 0.6 and 0.9 K on surface temperature. [20] also reported that this error strongly depends on the way atmospheric radiation is characterized and that it is very important to consider the atmospheric radiation in the same spectral range as the sensor (e.g. 10.5 µm – 12.5 µm, 8 µm – 14 µm…). This is particularly problematic since measuring the atmospheric radiation in a limited spectral range is complex.

In the present study, the method proposed by [20] for deriving surface temperature from thermal infrared measurements is re-assessed and tested on Landsat data acquired over the lower Rhône Valley in France (Avignon-Crau-Camargue area). The set of equations used for deriving atmospheric radiation is modified and a method for deriving surface emissivity in the Landsat thermal channel is presented. The method is evaluated by comparing surface temperatures derived from Landsat 7 – ETM+ images to ground measurements. The impact of the improvement of the atmospheric radiation and the surface emissivity estimation is assessed.

2. METHODS AND DATA

2.1. The relation between surface temperature and brightness temperature

Olioso (1995b) [20] proposed to estimate surface temperature (*Ts*) from top of canopy thermal infrared measurements (expressed as brightness temperature $Tb_{\lambda 1-\lambda 2}$, the temperature corresponding to a blackbody emitting the same radiation as the measured radiation) from an expression giving the temperature difference as:

$$Ts - Tb_{\lambda_1-\lambda_2} \cong \frac{\left(1-\varepsilon_{\lambda_1-\lambda_2}\right)}{4\,\varepsilon_{\lambda_1-\lambda_2}} Tb_{\lambda_1-\lambda_2} - \frac{\left(1-\varepsilon_{\lambda_1-\lambda_2}\right)}{4\,\varepsilon_{\lambda_1-\lambda_2}\, f_{\lambda_1-\lambda_2}\left(Tb_{\lambda_1-\lambda_2}\right)\sigma Tb_{\lambda_1-\lambda_2}^{\ 3}}\ Ra^{\downarrow}_{\lambda_1-\lambda_2} \qquad (1)$$

where the subscript λ_1–λ_2 refers to the considered spectral band, $\varepsilon_{\lambda 1-\lambda 2}$ is the surface emissivity in this band and $f_{\lambda 1-\lambda 2}(T)$ a factor corresponding to the fraction of energy emitted in this spectral band by a black body at temperature *T* relative to the emitted energy over the full spectrum. $Ra^{\downarrow}_{\lambda 1-\lambda 2}$ is the incident atmospheric radiation in the considered spectral band. The first term in Eq. 1 is an 'emissivity term' which increases with the reflectivity of the surface and with the temperature. The second term is a 'reflectivity term' which also increases with the surface reflectivity and the atmospheric radiation, but decreases with the temperature.

Considering Landsat-7 data, brightness temperatures ($Tb_{10.4-12.5\ \mu m}$) were obtained from the ETM+ thermal band in the

10.4–12.5 µm spectral range (band 6) after removing atmospheric effects using the atmospheric radiative transfer model MODTRAN ([3]). The factor $f_{10.4\text{-}12.5\ \mu m}(T)$ was expressed as (Idso 1981 [14]):

$$f_{10.4-12.5\,\mu m}(T) = -0.2338 + 0.2288 \cdot 10^{-2}\,T - 0.3617 \cdot 10^{-5} T^2 \quad (2)$$

It varies between 0.12 and 0.13 for temperatures between -10 ºC and +45 ºC. The incoming atmospheric radiation ($Ra^{\downarrow}_{10.4–12.5\mu m}$) can be expressed as a function of air temperature and a spectral atmospheric emissivity ($\varepsilon_{a\ 10.4–12.5\mu m}$) as given by [14]:

$$Ra^{\downarrow}_{10.4-12.5\,\mu m} = \varepsilon_{a\ 10.4-12.5\,\mu m} \cdot\ f_{10.4-12.5\,\mu m}(T_a) \cdot \sigma \cdot {T_a}^4 \quad (3)$$

The atmospheric emissivity was originally estimated from air temperature and air vapour pressure using formulas derived by [14] (see [20], [11]). However, [14] derived these formulas from measurements using a thermal infrared radiometer facing the zenith and receiving radiation from approximately two degree viewing angle. [23] showed that such measurements were not representative of the emission of the whole sky-hemisphere and that the emissivity expression provided by [14] should be corrected so that

$$\varepsilon_{a\ 10.4-12.5\,\mu m} = \gamma_{10.4-12.5\,\mu m} \cdot 5.91 \cdot 10^{-6} \cdot e_a \cdot exp\left(\frac{2450}{T_a}\right) \quad (4)$$

[12] provided an expression of the correction factor ($\gamma_{10.4–12.5\mu m}$) depending on the atmospheric precipitable water (W) that we adapted for ETM+ : $\gamma_{10.4-12.5\,\mu m} = 1.67 - 0.09\,W$. In our study, W was obtained as the mean of the values given at 12:00 UTC both by the local-radiosonde profiles made at Nîmes airport and the NCEP atmospheric provided by the operational atmospheric-correction tool available at http://atmcorr.gsfc.nasa.gov. In our conditions $\gamma_{10.5–12.5\mu m}$ ranged from 1.37 (for the wettest atmosphere) to 1.63 (for the driest atmosphere).

2.2. Estimation of surface spectral emissivity

Surface emissivity can be estimated from NDVI using relationships such as provided by van de Griend and Owe 1993 [27]: see for example [2]. Actually, as shown by Olioso (1995a, [19]), this relationship is only appropriate for regions similar to that used by [27] (i.e., a semi-arid region in Botswana). The variability of the relationship was analyzed through radiative transfer modeling in vegetation canopy by [19]. Wittich (1997) [29] proposed a simple analysis that made it possible to derive a simple and generic formula:

$$\varepsilon_{\lambda_1-\lambda_2} = \varepsilon_{\infty\,\lambda_1-\lambda_2} - \left(\varepsilon_{\infty\,\lambda_1-\lambda_2} - \varepsilon_{s\,\lambda_1-\lambda_2}\right)\left(\frac{NDVI-NDVI_\infty}{NDVI_s-NDVI_\infty}\right)^{k_2/k_1} \quad (6)$$

where *NDVI* is the normalized difference vegetation index defined from NIR and red reflectances (bands 4 and 3 on ETM+). This relationship can be applied to any study site as soon as its parameters can be derived from information on soil and plant canopy in the area of interest: $\varepsilon_{s10.4–12.5\mu m}$, $\varepsilon_{\infty 10.4–12.5\mu m}$, $NDVI_s$, $NDVI_\infty$, k_1 and k_2. The subscript s stands for bare soil conditions and the subscript ∞ stands for maximal *NDVI* at full vegetation cover. The coefficient k_1 is an attenuation factor relevant to the relation between *LAI* and *NDVI* ([1]) and k_2 an attenuation coefficient relevant to the relation between emissivity and *LAI* [19]. In our study, specific values for the parameters were derived from the analysis of the shape of the *NDVI* – emissivity relationship together with measurements of soil (at different moisture content) and vegetation canopy emissivities performed in our study area ([7], [17], [18]). Additional experimental measurements of emissivity from crops at large *NDVI* were also considered, including emissivity of wheat ([22]), alfalfa ([8]), and rice ([9]) fields from other experimental sites. Soil data from [18] consisted in laboratory measurements of reflectance spectra between 0.4 µm and 14 µm. They were used to derive emissivity and *NDVI* values by applying the response functions of ETM+ in band 3, 4 and 6. All the other measurements were performed in-situ using various versions of the box method ([23]).

2.3. The experimental area and the data

The study region is located in the lower Rhône Valley, South Eastern France, including the Avignon area (43.92°N; 4.88°E; 32 m above sea level) and the Crau-Camargue area (50 km around 43.56°N; 4.86°E; 0 to 60 m above sea level). It is mainly a flat area which presents a wide variety of surfaces including dry and irrigated grasslands, wetlands and various crops. Climate is Mediterranean, with irregular precipitations (annual cumulative precipitation range between 350 mm and 1100 mm with an average close to 550 mm), long dry periods in spring and summer, and strong winds. The area is covered by a single Landsat-7 ETM+ image. A network of ground stations was deployed over different types of ecosystems to monitor surface energy balance and meteorological variables: (1) the Avignon site hosted a succession of arable crops (sorghum and durum wheat) cultivated over a 2 ha size field (see [4], [6], [10], [16], [30]); (2) the Coussouls site corresponded to a large and flat stony area covered by a specific dry grass ecosystem (locally named 'coussouls'); (3) the Domaine du Merle site composed of irrigated meadows; (4) the Tour du Valat site was located within the Rhône River delta (Camargue) on a Mediterranean saltmarsh scrubs area (see [13]).

Brightness temperatures were estimated from 29 Landsat-7 images acquired from 2007 to 2010. Atmospheric corrections were performed using MODTRAN and atmospheric information derived from nearby radiosoundings performed in Nimes (20 to 40 km away). Surface temperatures were derived by applying equation (1). These surface temperatures derived from Landsat were compared to surface temperatures derived from pyrgeometer measurements (Kipp and Zonen CNR1 sensors) applying equation (1) to the 5-50 µm spectral range at the four surface energy balance stations.

3. RESULTS

3.1. Differences between surface and brightness temperatures

The theoretical impact of atmospheric radiation and emissivity on the difference between surface and brightness temperature is given by Eq. (1). It is presented on Figure 1 at different level of atmospheric radiation, surface emissivity and temperature. The temperature difference increased when atmospheric radiation decreased, emissivity decreased or temperature increased. Differences up to 2 degrees can be reached when temperature is high and surface emissivity is 0.97. It can be up to 7 K for emissivity of 0.91.

3.2. Surface emissivity

The *NDVI* - emissivity relationship obtained for our area is presented on Figure 2. At low *NDVI*, variations in emissivity and

NDVI were related to the level of soil moisture content (see [18]). Soil emissivity derived from soil reflectance spectra ranged between ~0.965 for dry soils to ~0.985 for wet soils, in agreement with in-situ values by [7] and [17]. Vegetation emissivity at high vegetation cover ranged between ~0.975 and ~0.990 (NDVI ~0.9). Three *NDVI* – emissivity relationships were derived in order to account for the variability in *NDVI* and emissivities (see Figure 2).

3.3. Surface temperature

The comparison of surface temperatures derived from Landsat data to surface temperatures obtained from ground measurements is given in Figure 3, showing a general good agreement and a slight overestimation by Landsat (Root mean square error RMSE = 1.7 K and bias ME = 0.6 K). Some discrepancies occurred for the Avignon site which can be explained by the spatial heterogeneity of the target (as shown by the high standard deviation around each point) and for the Tour du Valat site at high temperature which can be explained by the limited knowledge on emissivity for this site (salty marshes with a high level of salt, temporary flooded and presenting non-green vegetation stands affecting the emissivity – NDVI relationship).

When the derivation of surface temperature was done using the original set of equations presented by [20], i.e. without accounting for the correction factor $\gamma_{10.4-12.5\mu m}$, the root mean square error and the bias were only slightly increased (RMSE = 1.8 K and ME = 0.8 K). When surface emissivity was estimated from the equation proposed by [27] instead of the equation calibrated over local information, RMSE and ME were significantly increased (RMSE = 2.4 K and bias ME = 1.5 K). These results can be explained on one hand by the limited variations of the incident atmospheric radiation in the situation of our measurements (the range of value is quite similar before and after correction between 10 W m^{-2} and 40 W m^{-2} despite a corrective factor varying between 0.5 and 1.5), and on the other hand by large differences in surface emissivity between the equation from [27] and the local equation.

4. CONCLUSION

Our study shows that in the conditions of our images, emissivity estimation had the largest impact on the temperature difference. However, Figure 1 shows that the atmospheric impact can be large, in particular for high level of radiation which may occur in summer when the atmosphere is warmer and the vapor pressure is higher. The procedure presented in this study is currently being implemented in a processing chain developed for mapping evapotranspiration.

This work was performed in the frame of the Sirrimed project (European FP7 financial support) and in the frame of the development of the EVASPA processing chain to produce evapotranspiration from remote sensing images.

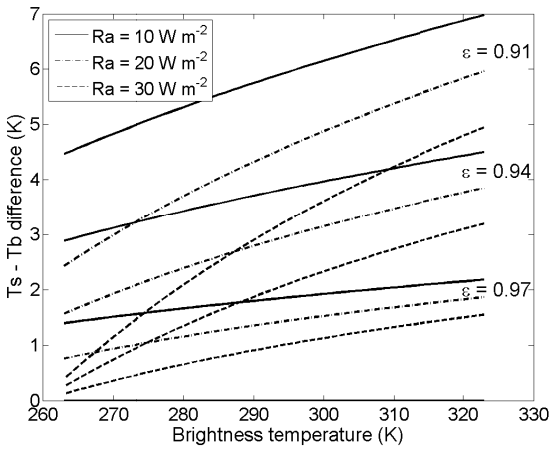

Figure 1. Differences between Landsat brightness temperature at the top of the canopy (Tb) and surface temperature (Ts) as a function of surface emissivity (ε), atmospheric radiation (Ra) and brightness temperature.

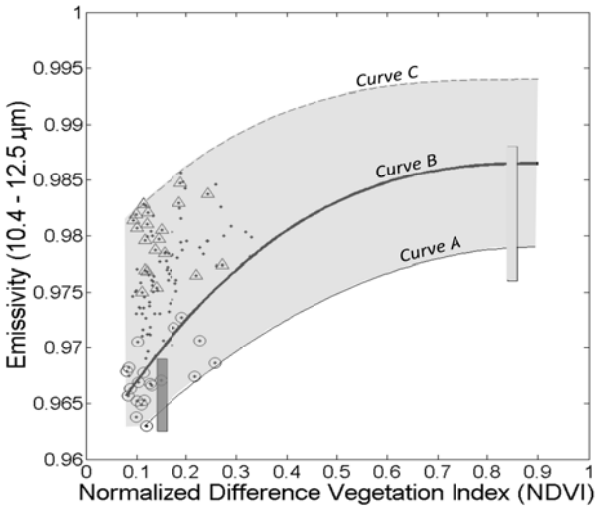

Figure 2. Relationship between *NDVI* and surface emissivity in the ETM+ band 6. Dots: values obtained from soil spectra acquired by [18]. Circles: for dry soils. Triangles: for wet soils. Vertical bars: range of in-situ values for bare soil (full bar) and vegetation (hatched bar). Curves A, B and C derived for accounting for variability in NDVI and emissivity with the following parameters:

	$\varepsilon_{s\,\lambda_1-\lambda_2}$	$\varepsilon_{\infty\,\lambda_1-\lambda_2}$	$NDVI_s$	$NDVI_\infty$	k_2/k_1
Curve A	0.963	0.980	0.079	0.9	2
Curve B	0.966	0.987	0.079	0.9	2.5
Curve C	0.981	0.995	0.120	0.9	3

4. REFERENCES

[1] Baret, F., Olioso, A., "Estimation à partir de mesures de réflectance spectrale du rayonnement photosynthétiquement actif absorbé par une culture de blé", *Agronomie*, 9, 885–895, 1989.

[2] Bastiaanssen, W.G.M., Menenti, M., Feddes, R.A., and Holtslag, A.A.M., "A remote sensing surface energy balance algorithm for land (SEBAL) - 1. Formulation", *Journal of Hydrology*, 213, 198-212, 1998.

[3] Berk, A., Anderson, G.P., Acharya, P.K., Hoke, M.L., et al., *MODTRAN4 Version 3 Revision 1 USERS MANUAL. AFRL Technical Report*, Hanscom AFB, USA, 2003.

[4] Boulet, G., Olioso, A., Ceschia, E., Marloie, O., et al., "An empirical expression to relate aerodynamic and surface temperatures for use within single-source energy balance models", *Agricultural and Forest Meteorology*, 161, 148-155, 2012.

[5] Carlson, T.N., Taconet, O., Vidal, A., Gillies, R.R., et al., "An overview of the workshop on thermal remote sensing held at La Londe les Maures, France, September 20-24, 1993", *Agricultural and Forest Meteorology*, 77, 141-151, 1995.

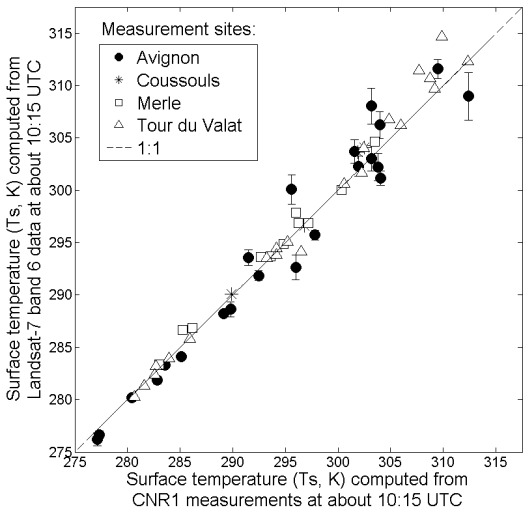

Figure 3. Comparison of surface temperature derived from Landsat and ground measurements (CNR1)

[6] Ceschia, E., Béziat, P., Dejoux, J.F., Aubinet, M., et al., "Management effects on net ecosystem carbon and GHG budgets at European crop sites", *Agriculture, Ecosystems and Environment*, 139, 363-383, 2010.

[7] Coll, C., Caselles, V., Rubio, E., Valor, E., et al., "Temperature and emissivity extracted from airborne multi-channel data in the ReSeDA experiment", *Agronomie*, 22, 567–573, 2002.

[8] Coll, C., Valor, E., Caselles, V., and Niclos, R., "Adjusted Normalized Emissivity Method for surface temperature and emissivity retrieval from optical and thermal infrared remote sensing data", *Journal of Geophysical Research-Atmospheres*, 108, D23, 4739, 2003.

[9] Coll, C., Galve, J.M., Sanchez, J.M., and Caselles, V., "Validation of Landsat-7/ETM+ thermal-band calibration and atmospheric correction with ground-based measurements", *IEEE Trans. Geoscience and Remote Sensing*, 48, 547-555, 2010.

[10] Delogu, E., Boulet, G., Olioso, A., Coudert, B., et al., "Reconstruction of temporal variations of evapotranspiration using instantaneous estimates at the time of satellite overpass", *Hydrology and Earth System Sciences*, 16, 2995–3010, 2012.

[11] Feijt, A.J., and Kohsiek, W., "The effect of emissivity variation on surface temperature determined by infrared radiometry", *Boundary-Layer Meteorology*, 72, 323-327, 1995.

[12] García-Santos, V., Valor, E., Caselles, V., Mira, M., et al., "Evaluation of different methods to retrieve the hemispherical downwelling irradiance in the thermal infrared region for field measurements", *IEEE Transactions on Geoscience and Remote Sensing,* 51, 2155-2165, 2013.

[13] Gallego-Elvira, B., Olioso, A., Mira, M., Reyes-Castillo, S., et al., "EVASPA (EVApotranspiration assessment from SPAce) tool: an overview", *Procedia Environmental Sciences*, under press, 2013.

[14] Idso, S.B., "A set of equations for full spectrum and 8 to 14 µm and 10.4–12.5 µm thermal radiation from cloudless skies", *Water Resources Research*, 17(2), 295–304, 1981.

[15] Idso, S.B., and Jackson, R.D., "Significance of fluctuation in sky radiant emittance for infrared thermometry", *Agronomy Journal*, 60, 388-392, 1968.

[16] Kutsch, W.L., Aubinet, M., Buchmann, N., Smith, P., et al., "The net biome production of full crop rotations in Europe", *Agriculture, Ecosystems and Environment*, 139, 336-345, 2010.

[17] Labed, J., and Stoll, M.P., "Spatial variability of land surface emissivity in the thermal infrared band: spectral signature and effective surface temperature", *Remote Sensing of Environment*, 38, 1–17, 1991.

[18] Lesaignoux, A., Fabre, S. and Briottet, X., "Influence of soil moisture content on spectral reflectance of bare soils in the 0.4–14 µm domain", *International Journal of Remote Sensing* , 34, 2268-2285, 2013.

[19] Olioso, A., "Simulating the relationship between thermal emissivity and the normalized difference vegetation index", *International Journal of Remote Sensing*, 16, 3211–3216, 1995a.

[20] Olioso, A., "Estimating the difference between brightness and surface temperatures for a vegetal canopy", *Agricultural and Forest Meteorology*, 72, 237–242, 1995b.

[21] Olioso, A., Chauki, H., Courault, D., and Wigneron, J.-P., "Estimation of evapotranspiration and photosynthesis by assimilation of remote sensing data into SVAT models", *Remote Sensing of Environment*, 68, 341-356, 1999.

[22] Olioso, A., Soria, G., Sobrino, J., and Duchemin, B., "Evidence of low land surface thermal infrared emissivity in the presence of dry vegetation", *IEEE Geoscience and Remote Sensing Letters*, 4, 112-116, 2007.

[23] Rubio, E., Caselles, V., and Badenas, C., "Emissivity measurements of several soils and vegetation types in the 8–14 µm wave band: Analysis of two field methods", *Remote Sensing of Environment*, 59, 490– 521, 1997.

[24] Sobrino, J.A., Gómez, M., Jiménez- Muñoz, J.C., Olioso, A., and Chehbouni, G., "A simple algorithm to estimate evapotranspiration from DAIS data : Application to the DAISEX campaigns", *Journal of Hydrology*, 315, 117-125, 2005.

[25] Svendsen, H., Jensen, H.E., Jensen, S.E., and Morgensen, V.O., "The effect of clear sky radiation on crop surface temperature determined by thermal thermometry", *Agricultural and Forest Meteorology*, 50, 329-243, 1990.

[26] Taconet, O., Olioso, A., Ben Mehrez, M., and Brisson, N., "Seasonal estimation of evaporation and stomatal conductance over a soybean field using surface infrared temperature", *Agricultural and Forest Meteorology*, 73, 321-337, 1995.

[27] Van de Griend, A., and Owe, M., "On the relationship between thermal emissivity and the normalized difference vegetation index for natural surfaces", *International Journal of Remote Sensing*, 14, 1119-1131, 1993.

[28] van der Kwast, J., Timmermans, W., Gieske, A., Su, Z., et al., "Evaluation of the Surface Energy Balance System (SEBS) applied to ASTER imagery with flux-measurements at the SPARC 2004 site (Barrax, Spain)", *Hydrology and Earth System Sciences*, 13, 1337-1347, 2009.

[29] Wittich, K.P., "Some simple relationships between land-surface emissivity, greenness and the plant cover fraction for use in satellite remote sensing". *International Journal of Biometeorology*, 41, 58–64, 1997.

[30] Zhao, Y., Ciais, P., Peylin, P., Viovy, N., et al., "How errors on meteorological variables impact simulated ecosystem fluxes: a case study for six French sites", *Biogeosciences*, 9, 2537–2564, 2012.